PB86-118460

Analysis of Regional Visibility in the Southwest Using Principal Component and Back Trajectory Techniques

(U.S.) Environmental Monitoring Systems Lab.
Las Vegas, NV

1985

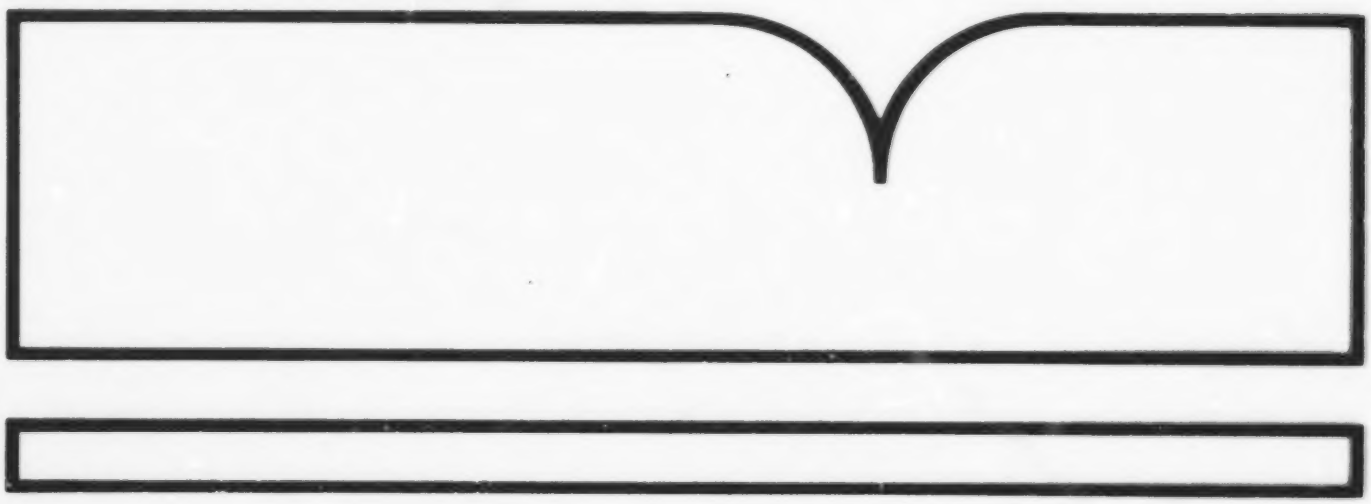

U.S. Department of Commerce
National Technical Information Service
NTIS

TECHNICAL REPORT DATA
(Please read Instructions on the reverse before completing)

1. REPORT NO.	2.	3. PB86-118460
EPA/600/J-85/225		

4. TITLE AND SUBTITLE
ANALYSIS OF REGIONIAL VISIBILITY IN THE SOUTHWEST USING PRINCIPAL COMPONENT AND BACK TRAJECTORY TECHNIQUES (Journal Version)

5. REPORT DATE
1985

6. PERFORMING ORGANIZATION CODE

7. AUTHOR(S)
M. Pitchford, A. Pitchford

8. PERFORMING ORGANIZATION REPORT NO.

9. PERFORMING ORGANIZATION NAME AND ADDRESS
A. Pitchford, EMSL-Las Vegas, U.S. EPA
P.O. Box 15027, Las Vegas, NV 89114

M. Pitchford, On assignment from National Oceanic & Atmospheric Environment to U.S. EPA, EMSL-Las Vegas.

10. PROGRAM ELEMENT NO.

11. CONTRACT/GRANT NO.

12. SPONSORING AGENCY NAME AND ADDRESS
Environmental Monitoring Systems Laboratory-Las Vegas
Office of Research & Development
U.S. Environmental Protection Agency
P.O. Box 15027, Las Vegas, NV 89114

13. TYPE OF REPORT AND PERIOD COVERED
Journal Reprint

14. SPONSORING AGENCY CODE
EPA 600/J-85

15. SUPPLEMENTARY NOTES
Atmospheric Environment, Vol. 19, No. 8 pp. 1301-1316, 1985

16. ABSTRACT

Approximately 3 years of visibility data from a 13-station teleradiometer network in the southwest desert is the basis for the analysis presented. Principal component analysis is employed to identify regions of similarly varying visibility for the entire data set and by seasons. "North", "Center", and "South" regions are identified in each of the four seasons. These regions change their size, shape and location somewhat through the seasons and thus are referred to as groups with each group containing four seasonal regions. Distinctive mean visibility levels and variations characterize the three groups. Back trajectory-analysis techniques are developed to infer the nature and extent of influence of upwind areas on the three visibility groups. Two years of daily back trajectories indicate primary detrimental influence from the southwest for the "North" group and from the southeast for the "South". Areas influencing the "Center"-group visibility are a combination of those affecting the other two groups. A method to calculate transport extinction budgets is demonstrated for the three visiblity groups.

17. KEY WORDS AND DOCUMENT ANALYSIS

a. DESCRIPTORS	b. IDENTIFIERS/OPEN ENDED TERMS	c. COSATI Field/Group

REPRODUCED BY
NATIONAL TECHNICAL
INFORMATION SERVICE
U.S. DEPARTMENT OF COMMERCE
SPRINGFIELD, VA 22161

18. DISTRIBUTION STATEMENT	19. SECURITY CLASS *(This Report)*	21. NO. OF PAGES
RELEASE TO PUBLIC	UNCLASSIFIED	17
	20. SECURITY CLASS *(This page)*	22. PRICE
	UNCLASSIFIED	

EPA/600/J-85/225
JOURNAL ARTICLE

Atmospheric Environment Vol. 19, No. 8, pp. 1301–1316, 1985
Printed in Great Britain.

0004–6981/85 $3.00 + 0.00
Pergamon Press Ltd.

ANALYSIS OF REGIONAL VISIBILITY IN THE SOUTHWEST USING PRINCIPAL COMPONENT AND BACK TRAJECTORY TECHNIQUES†

M. PITCHFORD* and A. PITCHFORD

Environmental Monitoring Systems Laboratory, U.S. Environmental Protection Agency, Las Vegas, Nevada, U.S.A.

(*First received* 26 *March* 1984; *in revised form* 3 *January* 1985)

Abstract—Approximately 3 years of visibility data from a 13-station teleradiometer network in the southwest desert is the basis for the analysis presented. Principal component analysis is employed to identify regions of similarly varying visibility for the enitre data set and by seasons. 'North', 'Center' and 'South' regions are identified in each of the four seasons. These regions change their size, shape and location somewhat through the seasons and thus are referred to as groups with each group containing four seasonal regions. Distinctive mean visibility levels and variations characterize the three groups. Back trajectory-analysis techniques are developed to infer the nature and extent of influence of upwind areas on the three visibility groups. Two years of four daily back trajectories indicate primary detrimental influence from the southwest for the 'North' group and from the southeast for the 'South'. Areas influencing the 'Center'-group visibility are a combination of those affecting the other two groups. A method to calculate transport extinction budgets is demonstrated for the three visibility groups.

Key word index: Visibility, principal component analysis, factor analysis, back trajectory, trajectory, extinction budget.

INTRODUCTION

The visibility protection provisions of the Clean Air Act of 1977 (Sections 165 and 169A of Public Law 95-95) have spawned a number of visibility-monitoring programs. (Malm *et al.*, 1981; Blumenthal *et al.*, 1981; Allard *et al.*, 1982; Hansen and Watson, 1983; Hoffer *et al.*, 1981). One such program, the Visibility Investigative Experiment in the West (VIEW), is a co-operative effort of the U.S. EPA's Environmental Monitoring Systems Laboratory-Las Vegas and the National Park Service (NPS). Teleradiometry data were collected at NPS-managed lands throughout the southwestern U.S. A detailed description of the monitoring locations, operating procedures and data-handling techniques is available elsewhere (U.S. EPA, 1983; Malm *et al.*, 1983). Briefly, instantaneous measurements of contrast between targets and the sky at a wavelength of 550 nm (green) are made three times daily, 9 a.m., noon and 3 p.m. local time, using a manual teleradiometer. The data used in the following analysis consist of daily mean extinction coefficients calculated for each tree-covered target-sight path at 13 of the VIEW monitoring sites (See Fig. 1) for a period from summer 1978 to autumn 1981.

The purpose of the analysis presented in this paper is to simplify the visibility-data set by identifying groups of sites that are related using principal component analysis and then working with these grouped data to investigate the influence of transport using trajectory analysis. The technique of factor analysis by principal components (also called orthogonal function or eigenvector analysis) has been used to determine spatial patterns of meteorological (Walsh and Mostek, 1980; Horel, 1981; Kutzback, 1970; Kidson, 1975) and air pollutant parameters (Ashbaugh *et al.*, 1984). Trajectory analysis has been used to estimate the movement of air pollutants (Hall *et al.*, 1973; Wolff *et al.*, 1977; Galvin *et al.*, 1978; Sampson *et al.*, 1981). When used to calculate the history of an air mass that arrived at a time and location of interest (back trajectory), it is a form of receptor modeling with which probable source regions influencing a receptor site can be identified (Pitchford *et al.*, 1981; Galvin *et al.*, 1978; Miller *et al.*, 1978; Raynor and Hayes, 1982).

DATA ANALYSIS

Principal component analysis

The first step in principal component analysis is the generation of a correlation matrix. Bivariate correlation coefficients of the daily mean extinction coef-

* On assignment from National Oceanic and Atmospheric Administration.

† Although the research described in this article has been funded wholly or in part by the United States Environmental Protection Agency, it has not been subjected to Agency review and therefore does not necessarily reflect the views of the Agency and no official endorsement should be inferred.

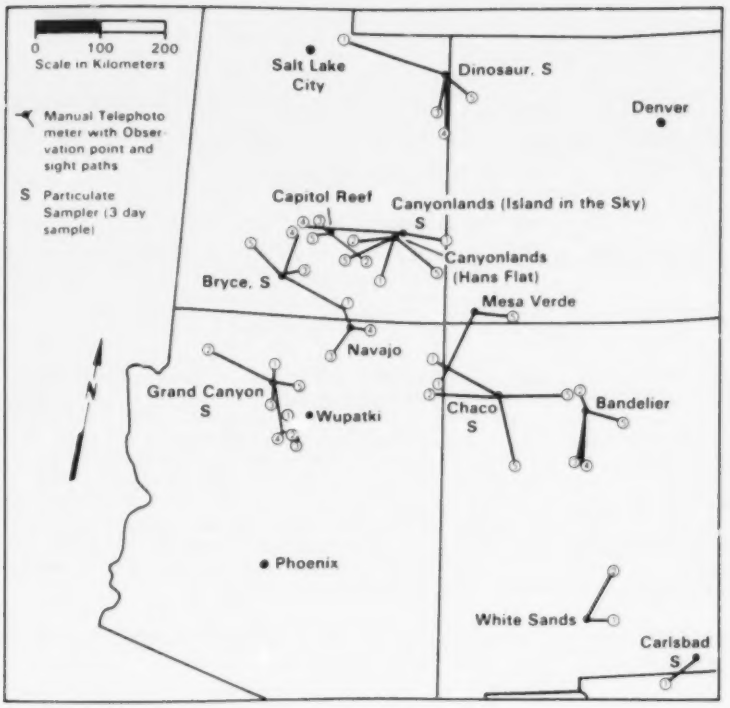

Fig. 1. 'VIEW' Monitoring network site map. [A list of sites, target names and distances to targets is available in Pitchford *et al.* (1981)].

ficients for each pair of teleradiometer sites were calculated by season and for the entire period of record. Table 1 shows the correlation matrix for all data. The typical number of data pairs is about 100 in the seasonal analysis and about 400 for the entire data record, although these values varied considerably depending on the sites paired. It was necessary to remove the Dinosaur, Canyonlands-Island in the Sky, Wupatki and Carlsbad sites from the winter-data set to eliminate an inconsistent correlation-coefficient matrix caused by substantial amounts of missing data for those sites.

Principal component analysis performed on the resulting correlation matrices using a commercially available computer routine (Dixon and Brown, 1977) produced a total of 16 significant factors. The varimax method of orthogonal rotation was employed to produce eigenvalues which tend to minimize intermediate factor-loading values thus simplifying physical interpretation (Horel, 1981). Table 2 contains the factor loadings for each site and factor and the percent variance explained by each factor. Hand-drawn factor-loading contour maps were constructed to display resulting geographic patterns for each factor. The two factors resulting from analysis of all data defined a northwestern (factor 1) and southeastern (factor 2) pattern. Inspection of the factor-loading contour maps for seasonally segregated data resulted in the identification of three regions (called the 'North', 'Center' and 'South' regions) which appeared in each season. By superimposing their 0.6 contour lines, the regions are shown to change their apparent location, shape and size somewhat as they progress through the seasons (Figs 2a–c), hence they are referred to as the 'North', 'Center' and 'South' groups (each group contains four seasonal regions). The two remaining factors may be part of an 'East' group which is only apparent by these data in the spring and autumn (see Fig. 2d). As a result of the greater uncertainty of an 'East' group, it will be dropped from subsequent analysis.

The temporal behavior of each factor was investigated by calculating its daily factor score (a standardized variable; mean, 0; S.D., 1). Since factor-score calculations require data for each site, missing data were estimated, where possible, by least-squares linear regression between pairs of related sites ($r \geqslant 0.5$). If the extent of the missing data was such that less than 75% of the contribution to the factor score was available, no factor-score value for the day was calculated. Inspection of factor-score time-plots for factors 1 and 2 for all data indicates that the short-term variations (generally less than 1 week) are of greater magnitude than any seasonal or year-to-year variations. The standard variable nature of factor scores prevented their being used to assemble visibility group ('North', 'Center' and 'South') composite time-plots for comparison of short- and long-term variations.

In order to investigate longer term variations for the

Table 1. Correlation coefficients (and numbers of data pairs) for all data

Site	Dinosaur	Capitol Reef	Can. I.S.	Can. H.F.	Bryce Canyon	Navajo	Mesa Verde
Dinosaur	1.000(603)						
Capitol Reef	0.444(558)	1.000(917)					
Can. I.S.	0.332(413)	0.371(660)	1.000(713)				
Can. H.F.	0.431(292)	0.585(425)	0.554(384)	1.000(509)			
Bryce Canyon	0.407(463)	0.597(731)	0.381(628)	0.474(471)	1.000(849)		
Navajo	0.351(460)	0.442(704)	0.442(628)	0.485(439)	0.540(720)	1.000(828)	
Mesa Verde	0.359(475)	0.256(729)	0.305(630)	0.410(458)	0.391(739)	0.424(741)	1.000(862)
Grand Canyon	0.324(530)	0.379(798)	0.339(654)	0.408(458)	0.547(775)	0.593(760)	0.411(809)
Wupatki	0.046(433)	0.227(665)	0.230(591)	0.373(362)	0.328(615)	0.384(625)	0.237(658)
Chaco Canyon	0.084(448)	0.193(628)	0.274(522)	0.304(418)	0.292(608)	0.429(630)	0.281(659)
Bandelier	0.063(481)	0.128(743)	0.229(633)	0.236(427)	0.221(705)	0.290(721)	0.367(763)
White Sands	0.084(513)	0.162(774)	0.151(639)	0.164(459)	0.245(738)	0.208(744)	0.269(778)
Carlsbad	0.002(271)	0.057(312)	0.186(214)	0.112(195)	0.142(234)	0.218(244)	0.004(255)

Site	Grand Canyon	Wupatki	Chaco Canyon	Bandelier	White Sands	Carlsbad
Grand Canyon	1.000(934)					
Wupatki	0.367(684)	1.000(731)				
Chaco Canyon	0.286(670)	0.228(548)	1.000(744)			
Bandelier	0.248(785)	0.217(615)	0.307(655)	1.000(866)		
White Sands	0.236(819)	0.150(662)	0.205(678)	0.440(785)	1.000(971)	
Carlsbad	0.265(275)	0.167(256)	0.351(279)	0.401(275)	0.593(363)	1.000(371)

Table 2. Factor loadings and percent variance explained (values less than 0.4 are deleted)

Site	Annual 1	Annual 2	Spring 1	Spring 2	Spring 3	Spring 4	Summer 1	Summer 2	Summer 3	Autumn 1	Autumn 2	Autumn 3	Autumn 4	Winter 1	Winter 2	Winter 3
Dinosaur	0.667		0.889				0.605			0.695				—	—	—
Can. I.S.	0.620		0.730				0.575			0.640				—	—	—
Can. H.F.	0.778		0.505	0.705			0.773			0.735						0.873
Capital Reef	0.751		0.648		0.401		0.803			0.863				0.472		0.710
Bryce Canyon	0.753		0.628		0.498		0.796			0.820				0.862		
Mesa Verde	0.567		0.456	0.464				0.499				0.757		0.476	0.614	
Navajo	0.711		0.404		0.613			0.655		0.629			0.450	0.788		
Grand Canyon	0.641				0.866		0.442	0.561		0.629				0.728		
Wupatki	0.408				0.479			0.739					0.798			
Chaco Canyon		0.509		0.753		0.412		0.599				0.520	0.594	—	—	—
Bandelier		0.702		0.781				0.437	0.527		0.680	0.469			0.717	
White Sands		0.767				0.694			0.795		0.896				0.736	
Carlsbad		0.829				0.914			0.813		0.865			—	0.712	—
% Variance	31.7	19.0	22.2	17.4	15.8	15.6	23.2	19.1	14.4	29.7	16.8	12.4	12.1	26.6	22.7	18.1

three groups identified above, another set of parameters was developed. The daily extinction values for sites with greater than 0.6 factor score were averaged to estimate an extinction coefficient value corresponding to each seasonal factor for each day. These were called factor mean extinction coefficients. The factor mean extinction coefficients are highly correlated with the corresponding factor-score values (for the 14 seasons $\bar{r} = 0.88$, with the lowest $r = 0.72$) and they maintain, in an absolute sense, the central tendency and variation information not available in the factor score values. Group mean extinction coefficients are the composites

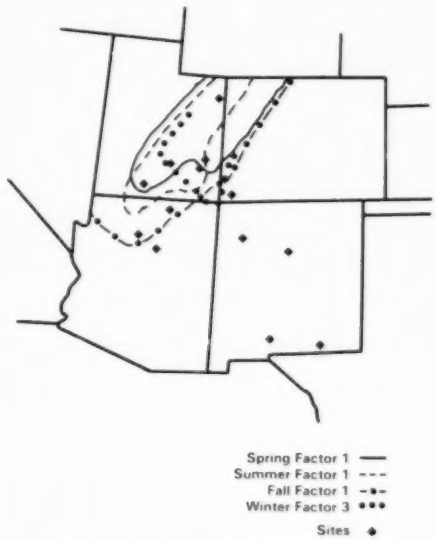

Fig. 2(a). 'North' group 0.6 contour lines.

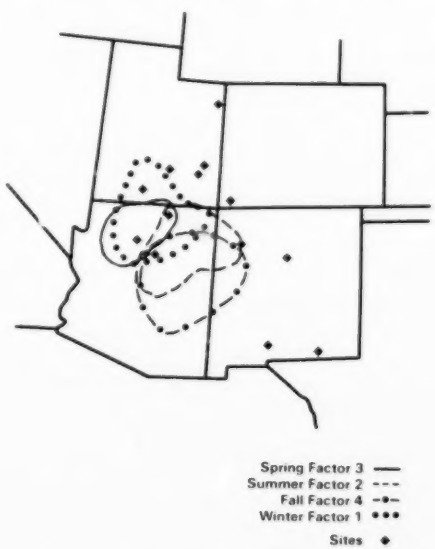

Fig. 2(b). 'Center' group 0.6 contour lines.

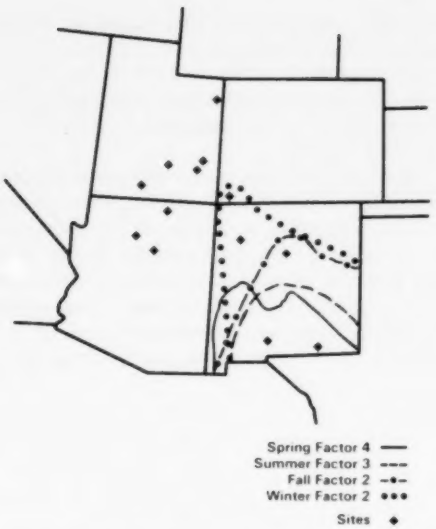

Fig. 2(c). 'South' group 0.6 contour lines.

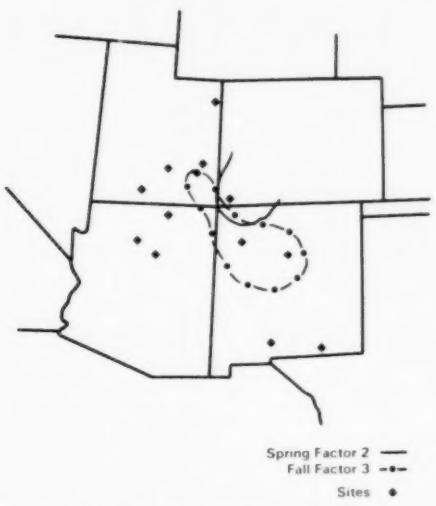

Fig. 2(d). 'East' group 0.6 contour lines.

of the appropriate factor mean extinction coefficients. Figures 3(a)–(c) show the time plots of the monthly average 'North', 'Center' and 'South' groups' mean extinction coefficients. The 'North' group has the highest overall visibility (lowest extinction coefficients) and no discernable annual cycle. 'Center' and 'South' groups have striking annual cycles. Poorest overall visibility is characteristic of the 'South' while the 'Center' has overall visibility between that of 'North' and 'South'. In spite of this, the large annual variation of the 'Center' group allows its winter months' visibility to exceed that of all the other groups.

Daily group mean extinction coefficients, b_{ext}, were divided into five classifications based on their magnitude. The classifications for each group were defined in terms of the number of standard deviations, S.D. (b_{ext}), from the mean of the group mean extinctions, b_{ext}. Table 3 shows the classification system. In order to avoid a seasonal bias caused by having an unequal number of each season, the classification system was applied to 2 full years of data (October 1979–September 1981). Table 4 shows the monthly distribution of each class. The scarcity of highest and high-visibility days in summer and lowest and low in the winter is apparent in all groups. These classifications provide a mechanism to link the results of the principal component analysis to the trajectory analysis.

Trajectory analysis

To calculate trajectories, a version of the Air Research Laboratory Atmospheric Transport and Dispersion (ATAD) Model was used (Heffter, 1980). The model uses data from upper-air soundings to determine transport-layer height and corresponding air trajectories. This version calculated four daily (every 6 h), 5-day back trajectories. Insufficient meteorological data causes some trajectory calculations to be terminated short of the nominal 5 days. For this work only trajectories of greater than 2 days were used. The output from the model is the position (longitude/latitude) of the air mass at 6-h increments. Tracer techniques have been employed to verify the utility of the ATAD model for specific trajectories in the eastern U.S. by Heffter and Ferber (1977) and by Raynor *et al.* (1983).

The application of the ATAD model in this work involved the calculation of nearly 10,000 trajectories. Thus a scheme was developed to summarize and evaluate trajectory information in place of plotting each trajectory. Miller (1981a,b) classified 5 years of trajectories at two locations by counting the occurrence of trajectories in wedge-shaped areas at various directions from the trajectory end point. After dividing the map into a regular grid (1° longitude × 1° latitude), Ashbaugh (1983) mapped the amount of time air parcels spent in each grid area as a means to identify and compare the sources of high-sulfur particulate concentrations. The technique employed in the present work involves determining the amount of time air parcels spend in each of 16 rectangular areas (called windows) as shown in Fig. 4. The areas were selected as representative of several major source regions and geopolitical areas of interest. Each point on the map is in two of the defined areas (one of the four quadrants and one other window). The following analysis is based upon the premise that the influence of an area (window) on the air quality of an air parcel moving over it is related to the length of time the air spends over the area.

Back trajectory end-point locations used in this work are Canyonlands National Park, Utah representing 'North' group, Carlsbad National Park, New Mexico representing the 'South' group and representing the 'Center' group are Grand Canyon National

Park, Arizona for winter and spring seasons and Petrified Forest National Park, Arizona (located 220 km southwest of the Grand Canyon site) for summer and autumn seasons. The large annual shift in the position of the 'Center' group prevented any fixed location from being representative.

For each day, the time in hours that an air parcel spent in each window was calculated by:

$$t_{ijk} = N_{ijk}/2,$$

where N_{ijk} is the number of trajectory segment end points (position of the trajectory every 30 min found by linear interpolation between 6-h time increments) in window i for group j and visibility classification k. To investigate trajectories without regard to visibility classifications (all data), it is useful to calculate t_{ij} using the equation above without the k subscripts. 'Center' group data sets were obtained by a simple composite of the data from the two endpoint locations for the appropriate seasons.

Table 5 contains daily mean values and corresponding standard errors of the mean of t_{ijk} for days sorted by visibility classification and for all data. Comparing the t_{ijk} values for the three visibility groups in this trajectory climatology table reveals several interesting features. Looking first at the 'all data' values indicates that the most dramatic differences in transport influences are between the 'North' and 'South' groups. As

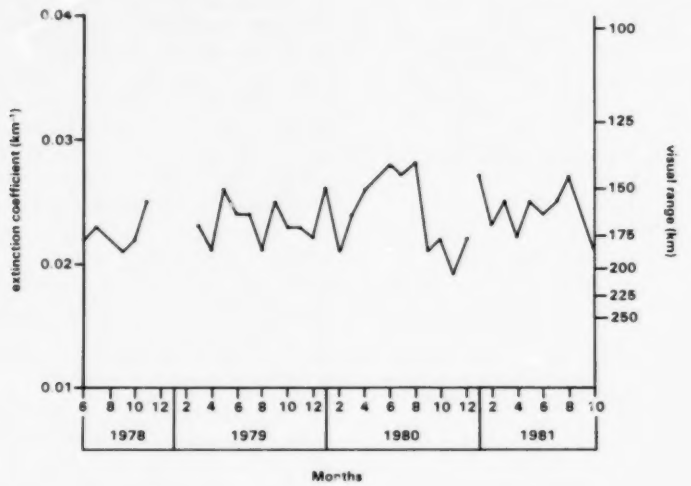

Fig. 3(a). Time-plot of monthly 'North' group mean extinction coefficients.

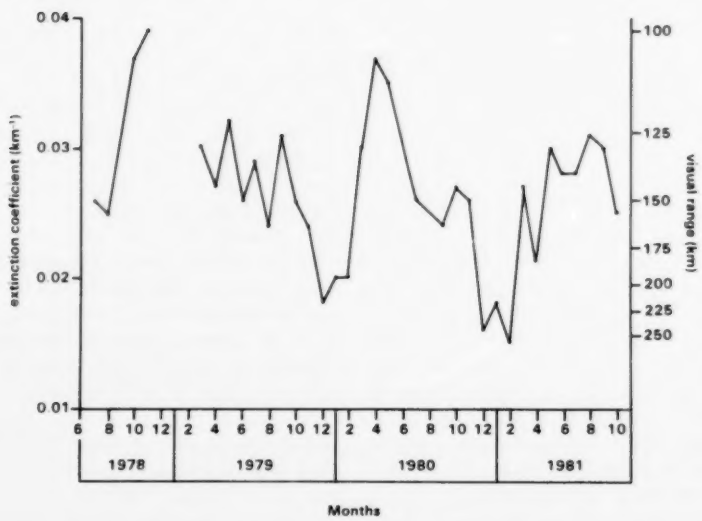

Fig. 3(b). Time-plot of monthly 'Center' group mean extinction coefficients.

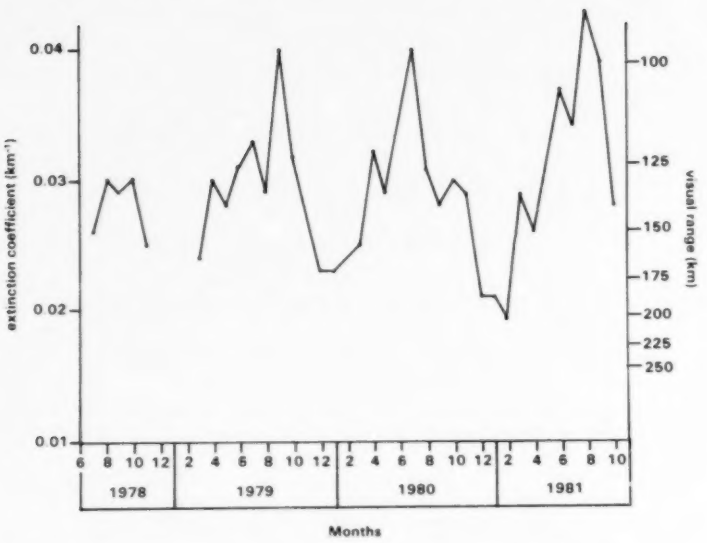

Fig. 3(c). Time-plot of monthly 'South' group mean extinction coefficients.

Table 3. Group mean extinction-coefficient classifications

Name*	Definition
Lowest	$b_{ext.} \geq \bar{b}_{ext.} + \text{S.D.}(b_{ext.})$
Low	$\bar{b}_{ext.} + \text{S.D.}(b_{ext.}) > b_{ext.} \geq \bar{b}_{ext.} + 0.5\text{S.D.}(b_{ext.})$
Average	$\bar{b}_{ext.} + 0.5\text{S.D.}(b_{ext.}) > b_{ext.} \geq \bar{b}_{ext.} - 0.5\text{S.D.}(b_{ext.})$
High	$\bar{b}_{ext.} - 0.5\text{S.D.}(b_{ext.}) > b_{ext.} \geq \bar{b}_{ext.} - \text{S.D.}(b_{ext.})$
Highest	$\bar{b}_{ext.} - \text{S.D.}(b_{ext.}) > b_{ext.}$

* Note that classification names refer to visibility and are thus inversely related to extinction.

might be expected, the 'Center' is influenced by a combination of the areas that effect the other two groups. The 'North' is most influenced by areas to the west, especially the southwest, including SCN, NW, NAZ, SC and NCN windows. In terms of directions, the 'South' group is more evenly influenced. Thus compared with the 'North' group, there is greater influence from the east at the expense of the southwest. The SB, SE and SAN, windows are important to the 'South'. The 'Center' group combines these characteristics and is influenced by SCN, UT, SC, SAN and NW windows. The large times associated with the window containing the trajectory endpoint for each of the three groups (UT for 'North', NAZ for 'Center' and NM for 'South') is due to the obvious need for all trajectories to pass through the endpoint and is therefore not very enlightening.

A similar analysis of the lower visibility classifications in Table 5 shows many of the same features as seen above, though there are some changes of emphasis. The 'North' group has a somewhat greater influence from the southwest at the expense of the north. Lower visibility in the 'South' group is accompanied by a greater influence from the east (especially the southeast) at the expense of the west (especially the northwest). The 'Center' has greater influence from the southeast though not from the southwest. The higher visibility classifications of Table 5 show that on cleaner days for all groups trajectories are primarily from the west with the northwest being more influential than the southwest. The 'Center' is also influenced by the northeast. As might be expected, the 'average' classification values in Table 5 are similar to the 'all data' values.

By systematically examining the t_{ijk} values, it should be possible to identify windows whose greater or lesser influence corresponds to different visibility levels. To aid in this effort an enrichment ratio R_{ijk} was defined as:

$$R_{ijk} = t_{ijk}/t_{ij\text{ave}}$$

where $t_{ij\text{ave}}$ is the time an air parcel spends in windows i and groups j for the average classification. Values of R_{ijk} can vary from zero to infinity. Values of R_{ijk} near one indicate that air parcels arriving at the trajectory end point of interest during classification k spent about the same amount of time in window i as during average visibility conditions. Numbers much greater than/less than one indicate the air parcel spent an unusually great/small amount of time in window i. Error propagation techniques were used to determine a standard error, S.E._R, associated with each R_{ijk} (Bevington, 1969).

Table 6 contains the R_{ijk} values and the one standard deviation conservative limit of R_{ijk} ($R_{ijk} + \text{S.E.}_R$ for $R_{ijk} < 1$ or $R_{ijk} - \text{S.E.}_R$ for $R_{ijk} > 1$). Values less than one are displayed as fractions to facilitate comparisons to values greater than one (a value x is as unusual as $1/x$). For an enrichment ratio, R_{ijk}, to be considered significantly larger than one, its corresponding conservative

Table 4. Distribution of group mean extinction classifications September 1979 to August 1981

	January		February		March		April		May		June		July		August		September		October		November		December	
	1980	1981	1980	1981	1980	1981	1980	1981	1980	1981	1980	1981	1980	1981	1980	1981	1979	1980	1979	1980	1979	1980	1979	1980
North																								
Lowest	5	7	3	3	3	8	5	1	7	3	7	5	8	3	8	9	8	1	3	2	5	1	3	6
Low	4	2	0	0	2	3	6	3	5	7	11	1	8	4	7	5	1	2	0	3	2	1	1	0
Average	13	14	8	2	15	7	13	12	14	14	11	17	13	22	15	13	6	13	14	10	8	5	6	3
High	4	2	8	0	7	5	3	9	4	4	0	5	1	1	0	3	11	7	7	9	10	11	7	10
Highest	2	2	7	4	2	5	2	4	0	2	0	1	0	0	0	0	3	6	5	4	4	11	12	9
Center																								
Lowest	0	1	0	0	6	5	14	0	10	4	5	4	1	2	2	5	7	2	5	4	5	5	0	0
Low	2	1	1	0	3	4	5	1	4	3	5	4	5	2	1	7	5	3	1	1	1	1	1	0
Average	5	2	9	2	12	5	5	12	13	16	17	16	14	23	19	14	11	11	14	18	4	15	5	3
High	16	11	8	7	4	4	3	10	3	5	2	4	10	3	8	4	5	10	9	4	7	2	6	10
Highest	6	15	7	17	1	7	0	6	0	1	0	0	0	0	0	0	1	3	1	0	8	4	15	16
South																								
Lowest	0	0	3	0	0	4	3	1	2	4	9	11	15	6	3	12	11	3	5	4	1	4	1	0
Low	0	1	0	0	0	1	4	1	1	4	4	7	3	4	5	5	5	3	6	3	7	1	0	0
Average	9	5	6	1	15	8	19	12	19	18	10	10	10	14	16	7	12	11	11	14	10	14	8	7
High	14	10	8	6	10	12	2	14	8	4	3	0	1	2	1	1	0	10	5	7	7	3	13	12
Highest	6	14	10	19	3	1	0	1	0	0	0	0	1	0	1	0	0	1	3	1	4	5	7	10

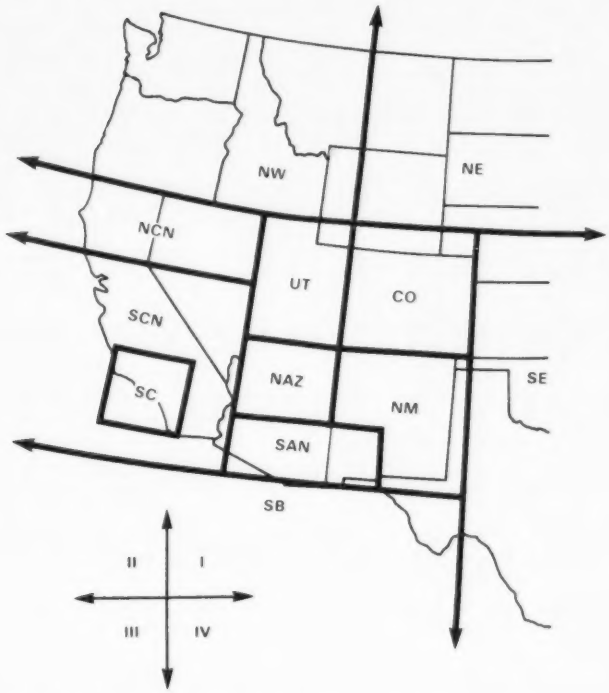

Fig. 4. Locations of the 16 windows. Windows include the four quadrants and 12 regions defined by lines of constant longitude and latitude. The intersection point of the quadrants, indicated at the bottom, is understood to be at the trajectory endpoint.

limit must also be larger than one. Similarly for R_{ijk} to be considered significantly less than one, its corresponding conservative limit must also be less than one.

Using the R_{ijk} values the beneficial or detrimental influence of the windows on visibility for the three 'groups' have been identified and are displayed in Table 6 on lines labeled 'influence'. If trajectories associated with good visibility spend more time in an area than trajectories associated with average visibility, a beneficial influence from the area can be inferred. An area would also have beneficial influence if trajectories associated with poor visibility spent less time in the area than trajectories associated with average visibility. For the purpose of the analysis in Table 6, windows with beneficial influence are defined to have enrichment ratios and conservative limits greater than 1.10 for highest and high-visibility classifications and/or enrichment ratios and conservative limits less than 1/1.10 for lowest and low classifications. Windows with detrimental influence are similarly defined with enrichment ratios and conservative limits greater than 1.10 for lowest and low classifications and/or less than 1/1.10 for highest and high classifications. For a few windows there were both beneficial and detrimental characteristics. In some of these instances, the enrichment ratio was small for both the higher and the lower visibility classifications. In other words trajectories spend less time in these windows for both visibility extremes than when associated with average visibility days. Since these windows favor average visibility they were labeled average influence. Several windows had influence that was undetermined because the enrichment ratios were not significantly different from one. This was either due to a high uncertainty in the enrichment ratios caused by few trajectories in the window or due to a lack of either beneficial or detrimental influence.

One of the more striking differences between the groups is the large number of windows with an apparent detrimental influence for the 'North' or 'Center' groups that are not detrimental for the 'South' group. This does not necessarily imply that these windows have considerably different influence, in an absolute sense, for the 'South' group. It may result from the use of group-mean and S.D. extinction coefficients to define the visibility classifications. Since the 'South' group has considerably lower visibility than the 'North' and 'Center' groups, extinction coefficients that would be classified as average visibility in the 'South' could be classified lowest or low visibility in the 'North' and 'Center' groups.

Using the t_{ij} values in Table 5 as a measure of the frequency of influence, along with the influence de-

Table 5. Mean duration and standard error of the mean in hours. Maximum possible hours is 480 (24 h day^{-1} × 4 trajectories day^{-1} × 5 days of back trajectory). *N* is number of days with trajectories of greater than 48 h

Visibility-group classification	Window I	II	III	IV	NCN	SC	SCN	NAZ	NM	SAN	UT	CO	NW	NE	SE	SB	Total	*N*
North																		
Lowest	26.76	87.32	217.87	24.21	14.61	31.96	91.07	41.66	9.15	14.26	104.04	11.76	24.97	6.66	1.51	4.61	356.16	102
	7.68	12.41	15.06	5.54	4.07	4.81	8.60	5.63	2.77	3.41	8.75	3.83	6.29	3.13	1.12	1.33	13.79	
Low	19.06	80.02	228.13	12.49	19.92	36.12	108.43	40.31	4.49	7.71	76.83	8.98	26.32	5.90	0.74	3.92	339.70	72
	7.15	14.72	19.44	6.26	5.91	6.21	10.72	6.55	2.73	2.30	7.95	3.58	7.53	3.03	0.74	1.31	17.49	
Average	29.24	117.37	205.12	14.07	27.94	35.79	88.39	34.67	3.92	11.29	94.41	13.36	43.62	9.08	0.48	2.98	365.79	242
	4.87	8.96	10.43	3.12	3.39	3.56	5.50	3.43	1.25	2.60	4.67	2.61	5.66	2.34	0.30	0.67	7.90	
High	77.62	136.13	143.58	18.36	25.84	23.44	64.95	21.50	2.06	2.52	92.81	44.25	72.19	24.47	0.14	1.88	375.68	116
	12.19	12.51	13.92	4.19	4.54	5.45	7.36	3.93	0.89	0.88	6.36	7.36	9.10	5.55	0.10	0.75	11.71	
Highest	23.10	209.79	116.02	9.67	43.46	7.41	61.80	17.16	0.87	1.74	118.18	11.69	90.11	4.88	0.00	1.41	358.58	71
	6.65	17.22	15.49	3.09	8.26	2.64	11.14	4.50	0.41	1.08	9.46	3.49	12.90	2.42	0.00	0.70	16.21	
All	36.19	122.32	187.69	15.90	26.15	29.46	83.60	31.93	4.15	8.55	96.43	18.31	49.37	10.76	0.57	2.97	362.10	603
	3.60	5.69	6.48	1.95	2.14	2.14	3.55	2.09	0.78	1.25	3.08	2.03	3.63	1.61	0.24	0.42	5.34	
Center																		
Lowest	33.42	128.41	125.65	58.55	18.37	29.07	69.01	77.99	20.05	36.10	22.54	4.64	32.97	5.75	15.63	13.89	346.03	71
	8.57	17.13	14.32	12.87	4.29	7.26	9.82	9.62	5.31	7.73	5.32	2.62	9.72	3.10	6.17	5.42	17.61	
Low	30.50	129.51	110.67	80.97	13.97	26.20	66.39	90.98	39.74	34.73	32.67	3.07	17.23	0.00	9.02	17.74	351.65	46
	8.85	20.40	14.42	18.70	5.02	6.99	11.66	13.41	11.13	8.12	12.34	2.89	8.41	0.00	4.39	6.76	22.99	
Average	41.08	129.00	147.02	39.42	17.34	33.20	86.56	82.64	21.04	29.42	26.41	11.76	20.42	4.86	9.25	13.62	356.51	218
	6.47	9.63	9.61	6.09	2.74	3.97	5.74	4.86	3.89	3.71	3.51	2.85	3.62	1.60	2.62	2.	9.04	
High	49.77	105.88	147.45	42.09	11.54	33.99	94.33	79.03	21.61	23.31	30.46	10.39	18.28	3.51	5.62	13.17	345.19	121
	9.03	10.17	12.16	8.76	2.16	5.18	8.08	6.32	4.56	3.93	4.66	3.23	4.21	1.57	2.51	3.55	12.70	
Highest	108.29	178.56	57.64	27.66	24.16	9.82	84.36	82.45	8.67	5.22	82.27	18.39	39.76	7.05	1.33	3.93	372.15	96
	13.86	14.42	9.28	6.73	4.43	2.82	11.30	6.93	3.03	2.14	9.54	4.58	7.18	3.19	0.93	2.65	13.36	
All	52.81	132.52	125.79	43.88	17.11	28.19	83.94	81.91	20.45	25.18	37.91	10.97	24.66	4.65	7.88	12.21	355.00	552
	4.37	5.85	5.55	4.03	1.58	2.30	3.84	3.13	2.24	2.15	2.85	1.61	2.57	0.99	1.48	1.64	5.88	
South																		
Lowest	90.32	55.61	60.95	138.66	1.01	1.21	15.72	4.38	63.34	22.20	7.69	5.91	2.24	9.87	152.49	59.55	345.53	93
	13.71	11.15	10.74	13.72	0.65	0.54	4.48	1.93	4.36	5.35	2.77	2.40	1.10	3.64	14.46	8.27	13.84	
Low	40.26	94.84	74.59	101.50	4.82	4.97	16.13	11.82	66.22	32.64	6.00	6.48	9.43	6.56	72.27	73.93	311.19	59
	9.42	17.64	13.53	14.72	3.83	2.55	4.96	3.68	8.05	6.84	2.77	2.61	3.35	2.78	12.17	9.98	18.33	
Average	50.14	118.37	81.02	61.57	3.67	7.55	17.52	11.92	73.45	34.50	9.39	15.11	8.68	12.40	50.80	66.20	311.09	215
	6.81	10.20	6.97	6.48	0.87	2.06	2.84	2.13	5.24	4.31	1.85	2.92	2.17	2.50	5.51	5.40	9.57	
High	35.67	161.86	85.46	22.96	4.71	3.93	16.27	13.46	72.37	31.50	18.93	27.17	19.56	10.63	25.18	62.37	305.95	123
	6.38	14.53	9.25	5.63	1.30	1.40	2.92	2.21	6.32	4.41	3.73	5.59	4.43	2.68	6.26	7.62	13.19	
Highest	23.45	214.27	76.01	33.81	8.94	9.82	24.00	17.00	89.21	40.68	28.83	29.55	16.23	10.76	24.77	47.29	346.91	77
	7.27	18.66	11.70	8.54	2.19	3.52	4.08	3.52	7.78	6.56	4.79	5.74	5.64	3.64	8.87	8.19	15.72	
All	48.94	128.09	77.34	66.13	4.29	5.76	17.69	11.70	72.94	32.48	13.47	17.28	11.09	10.77	60.62	62.51	320.50	567
	4.03	6.46	4.31	4.35	0.67	1.01	1.63	1.17	2.86	2.38	1.39	1.91	1.54	1.38	4.25	3.33	5.91	

Table 6. Enrichment ratio and one standard error conservative confidence limit, plus influence determination* for 'North', 'Center' and 'South' groups

Visibility-group classification	Window I	II	III	IV	NCN	SC	SCN	NAZ	NM	SAN	UT	CO	NW	NE	SE	SB
North																
Lowest	1/1.09	1/1.34	1.06	1.72	1/1.91	1/1.12	1.03	1.20	2.33	1.26	1.10	1/1.14	1/1.75	1/1.36	3.15	1.55
	1.16	1/1.22	1/1.02	1.04	1/1.67	1.01	1/1.08	1.01	1/1.46	1/1.13	1/1.00	1.13	1/1.53	1/1.01	1/−0.24	1/1.17
Low	1/1.53	1/1.47	1.11	1/1.13	1/1.40	1.01	1.23	1.16	1.15	1/1.46	1/1.23	1/1.49	1/1.66	1/1.54	1.54	1.32
	1/1.23	1/1.30	1.01	1.28	1/1.16	1/1.20	1.08	1/1.06	1/2.88	1/1.22	1/1.13	1/1.17	1/1.41	1/1.15	1/1.20	1/1.36
Average	1.00	1.00	1.00	1.00	1.00	1.00	1.00	1.00	1.00	1.00	1.00	1.00	1.00	1.00	1.00	1.00
High	2.65	1.16	1/1.43	1.30	1/1.08	1/1.53	1/1.36	1/1.61	1/1.90	1/4.48	1/1.02	3.31	1.65	2.69	1/3.43	1/1.59
	1.55	1.04	1/1.34	1/1.09	1.08	1/1.33	1/1.26	1/1.45	1/1.55	1/4.16	1.05	1.49	1.31	1.05	1/2.84	1/1.27
Highest	1/1.27	1.79	1/1.77	1/1.46	1.56	1/4.83	1/1.43	1/2.02	1/4.51	1/6.49	1.25	1.14	2.07	1/1.86	0.00	1/2.11
	1/1.03	1.53	1/1.64	1/1.19	1.10	1/4.50	1/1.27	1/1.79	1/4.08	1/5.92	1.13	1.10	1.45	1/1.47	1.00	1/1.71
Influence	B	B	D	D	B	D	D	D	D	A	B	B	B	A	D	D
Center																
Lowest	1/1.23	1/1.00	1/1.17	1.49	1.06	1/1.14	1/1.25	1/1.06	1/1.05	1.23	1/1.17	1/2.53	1.61	1.18	1.69	1.02
	1/1.02	1.13	1/1.07	1.00	1/1.25	1.07	1/1.13	1.05	1.19	1/1.11	1.03	1/2.07	1/1.18	1/2.33	1/1.78	1/1.63
Low	1/1.35	1.00	1/1.33	2.05	1/1.24	1/1.27	1/1.30	1.10	1.89	1.18	1.24	1/3.83	1/1.19	0.00	1/1.03	1.30
	1/1.11	1/1.18	1/1.21	1.08	1.04	1/1.05	1/1.15	1/1.08	1/1.12	1/1.17	1/1.52	1/3.07	1.19	1.00	1.44	1/1.52
Average	1.00	1.00	1.00	1.00	1.00	1.00	1.00	1.00	1.00	1.00	1.00	1.00	1.00	1.00	1.00	1.00
High	1.21	1/1.22	1.00	1.07	1/1.50	1.02	1.09	1/1.05	1.03	1/1.26	1.15	1/1.13	1/1.12	1/1.38	1/1.65	1/1.03
	1/1.06	1/1.13	1/1.09	1/1.20	1/1.34	1/1.16	1/1.01	1.03	1/1.24	1/1.11	1/1.05	1.13	1.08	1/1.05	1/1.29	1.22
Highest	2.64	1.38	1/2.55	1/1.43	1.39	1/3.38	1/1.03	1/1.00	1/2.43	1/5.64	3.30	1.56	1.95	1.45	1/6.95	1/3.47
	1.75	1.23	1/2.40	1/1.22	1.04	1/3.12	1.10	1.08	1/2.12	1/5.25	2.11	1/1.05	1.26	1/2.01	1/6.32	1/2.90
Influence	B	B/D	A	D	D	D	B	U	D	D	B	B	B	U	D	D
South																
Lowest	1.80	1/2.13	1/1.33	2.25	1/3.63	1/6.24	1/1.11	1/2.72	1/1.16	1/1.55	1/1.22	1/2.56	1/3.88	1/1.26	3.00	1/1.11
	1.31	1/1.95	1/1.17	1.75	1/3.09	1/5.82	1.13	1/2.34	1/1.09	1/1.35	1.06	1/2.21	1/3.44	1.03	2.15	1.01
Low	1/1.25	1/1.25	1/1.09	1.65	1.31	1/1.52	1/1.09	1/1.01	1/1.11	1/1.06	1/1.57	1/2.33	1.09	1/1.89	1.42	1.12
	1/1.05	1/1.09	1.07	1.25	1/−17.46	1/1.14	1.18	1.30	1.00	1.13	1/1.21	1/1.99	1/1.50	1/1.54	1.08	1/1.05
Average	1.00	1.00	1.00	1.00	1.00	1.00	1.00	1.00	1.00	1.00	1.00	1.00	1.00	1.00	1.00	1.00
High	1/1.41	1.37	1.05	1/2.68	1.28	1/1.92	1/1.08	1.13	1/1.01	1/1.10	2.02	1.80	2.25	1/1.17	1/2.02	1/1.06
	1/1.25	1.20	1/1.07	1/2.46	1/1.21	1/1.62	1.08	1/1.09	1.07	1.03	1.22	1.13	1.10	1.04	1/1.80	1.05
Highest	1/2.14	1.81	1/1.07	1/1.86	2.44	1.30	1.37	1.43	1.21	1.13	3.07	1.96	1.87	1/1.15	1/2.05	1/1.40
	1/1.87	1.52	1.07	1/1.63	1/1.02	1/1.44	1.05	1.01	1.09	1/1.05	1.50	1.21	1/1.53	1.12	1/1.75	1/1.25
Influence	D	B	B	D	B	A	U	B	U	B	B	B	B	B	D	D

* B, beneficial; D, detrimental; A, average; B/D, beneficial and detrimental; U, undetermined.

termination from Table 6, the relative importance of the various windows can be estimated. The 'North' group has its primary detrimental influence from the southwest (III, SCN and SC) with secondary detrimental influence from the southeast (IV, NAZ and SAN). The areas of primary detrimental influence for the 'Center' group are the southeast (IV and NM), the south coast urban area of California (SC) and the area of southern Arizona and New Mexico that contains the non-ferrous smelting industry (SAN). Northern California and Nevada (NCN) have secondary detrimental influence, while the area of Southern California and Nevada exclusive of the south coast urban area (SCN) has a major beneficial influence for the 'Center'. Both in terms of its frequency and association with lowest visibility, the 'South' group has primary detrimental influence from the east (IV, I and SE). Apparently the detrimental influence of the east on the 'South' group is primarily responsible for the low average visibility which causes those areas that are detrimental to the other two groups to be relatively beneficial to visibility for the 'South'. The area south of the border (SB) also has primary detrimental influence for the 'South'. However, unlike the windows to the east, its influence results from less time associated with the cleanest visibility.

The advantages of the analysis technique presented above are its use of elementary mathematics and relatively simple concepts to summarize trajectory information and relate it to air-quality parameters. The disadvantages are the qualitative nature of the results and the use of what amounts to a bivariate analysis technique where a multivariate technique is more appropriate. The following approach was developed to eliminate these disadvantages. This approach is similar to the one described above in that the amount of time an air parcel spends in each window is related to the visibility at the trajectory end point. However, the use of five visibility classifications and corresponding average t_{ijk} values is abandoned in favor of daily group mean extinction coefficients and corresponding t_{ij} values.

If it was assumed that the contribution from each window to the extinction coefficient at the trajectory end point was only dependent on the amount of time an air parcel spent in the window, then the rate of contribution by each window would be a constant. These constants could be determined by solving a set of simultaneous linear equations of the form:

$$b_{\text{ext},j} = \sum_{i=5}^{16} C_{ij} t_{ij},$$

where $b_{\text{ext},j}$ is the daily group mean extinction coefficient for group j and C_{ij} is the contribution rate term for window i and group j. Only the last twelve windows are chosen to avoid overlapping areas while providing coverage for every possible air parcel position. Thus in this idealized model only twelve days of visibility and trajectory data need to be evaluated to solve for the twelve C_{ij} terms. However, it is obvious that the contribution rate terms are not constant because of other influencing factors (e.g. precipitation events, relative humidity, varying source terms, etc.). There is also visibility-measurement uncertainty and uncertainty associated with trajectory calculations, all of which prevent an exact solution for this model.

Approaching the problem statistically allows the mean value and variability for each contribution rate term to be assessed. This is accomplished in spite of the confounding factors mentioned above by the addition of an error term ε, to the right-hand side of the expression above and the application of multiple linear regression with zero intercept to the resulting equation. C_{ij} terms are determined which result in the lowest mean value of ε^2 where the mean value of ε is assumed to be zero.

Figures 5(a–c) show the regression coefficients, C_{ij}, and their standard errors from the regression analysis. The relative influence of the windows on visibility for each group is related to the magnitude of the coefficients. The larger the value, the more detrimental is the influence. A comparison of these values with the influence determination of Table 6 generally shows good agreement, with only a few cases where one method indicates a detrimental while the other indicates a beneficial determination. For the 'North' group a regression coefficient value of 5 ($100{,}000\ \text{km}^{-1}\,\text{h}^{-1}$) separates the beneficial from the detrimental determinations of the earlier analysis. The only significant exception is for UT where the regression analysis would indicate detrimental influence. The enrichment-ratio-determined detrimental influence for the SC, NM and SE windows and the beneficial influence for the NCN windows are shown to have average or uncertain influence in Fig. 5(a). A similar comparison for the 'Center' group, using a value of about 4 ($100{,}000\ \text{km}^{-1}\,\text{h}^{-1}$), indicates two significant exceptions. In the earlier analysis the SCN and NW windows were beneficial while Fig. 5(b) indicates detrimental influence. The undetermined influence indicated for NAZ is shown to be detrimental by the linear regression method. Comparing the two analysis results for the 'South' group suggests a coefficient value of about 9 ($100{,}000\ \text{km}^{-1}\,\text{h}^{-1}$) to distinguish beneficial from detrimental. For the 'South' SC is shown in Fig. 5(c) to be beneficial not average and one of the two previously undetermined influence windows (SC) is better resolved while the uncertainty of others is shown. In cases of disagreement between the two techniques, the results from the regression analysis should be favored since the use of a multivariate analysis approach is more appropriate.

A conspicuous feature of the regression coefficients for each group when displayed as in these figures is that, with the exception of the SB window for the 'North' group, they all lie in a somewhat narrow range from 2 to 12 ($100{,}000\ \text{km}^{-1}\,\text{h}^{-1}$). Many of the coefficients are statistically similar at the one standard error level. Thus there appears to be two or at most

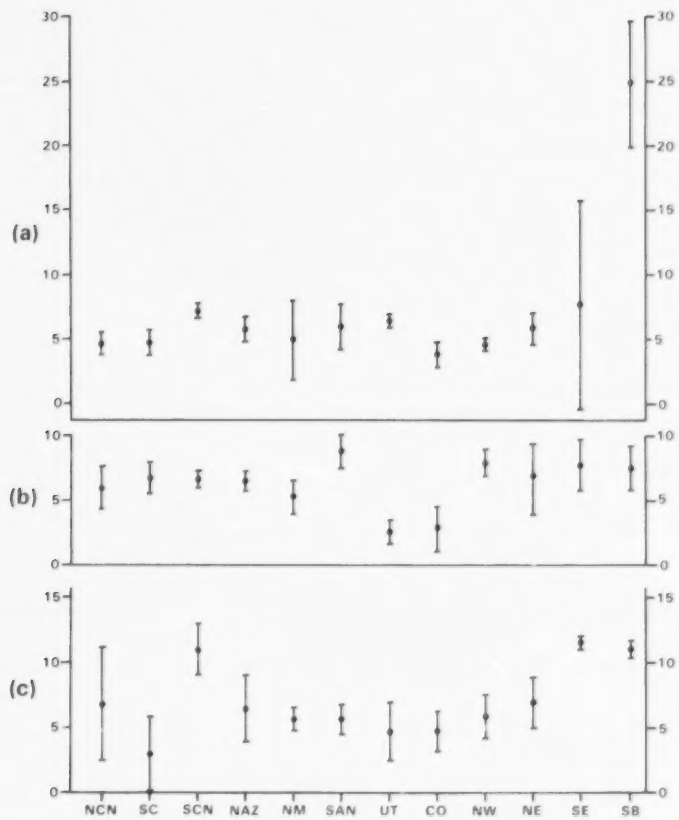

Fig. 5(a–c). Coefficients and standard errors (100,000 km^{-1} h^{-1}) from regression analysis for 'North', 'Center' and 'South' groups, respectively.

three distinguishable sets of regression coefficients for each group.

It may seem physically unreasonable for areas with large differences in source intensity to produce similar extinction per unit residence time. There are two factors which make this intuitive argument not compelling. The first has to do with the nature of emissions from the areas. It is certainly reasonable that some of the areas or windows have much greater anthropogenic emissions than others (this was by design). However, the analysis considers the total effect of an area. It does not distinguish anthropogenic from natural sources of degraded visibility. The latter includes vegetative organic and crustal materials plus the greater scattering efficiency caused by higher relative humidity.

The other factor concerns the processes at work during transport. Obviously within, or close to, and directly downwind from a large source, the extinction would be well above natural or background levels. It is also true that analysis of the worst-visibility days often suggests transport from distant major sources. However, it is not reasonable to conclude that high-pollutant levels will always survive dispersion and deposition mechanisms during transport from distant source areas. In fact earlier work (Pitchford *et al.*, 1981) using trajectories showed that 3 of the 10 best-visibility days for Grand Canyon are associated with paths going directly over the Los Angeles urban area. The analysis in the present work is applied to 2 years of data. Thus, the dramatic worst-day situations are diluted with hundreds of other days to provide information on the so-called average day.

The near pristine conditions of the average-day visibility and pollutant levels in these remote areas lends credence to the two arguments discussed above. Certainly at these rather clean pollutant levels there is relatively high contribution by natural causes of visibility degradation which are a minor component in more polluted areas. It is also obvious that the high levels of pollutants emitted from distant locations must be substantially diminished during transport.

The products, $C_{ij}t_{ij}$, are the regression-model-estimated contributions to extinction by window i for group j. Figures 6(a–c) are transport-extinction budget pie diagrams showing the mean contributions for the two years of trajectory data for the 'North', 'Center' and 'South' groups. Notice that for each group the

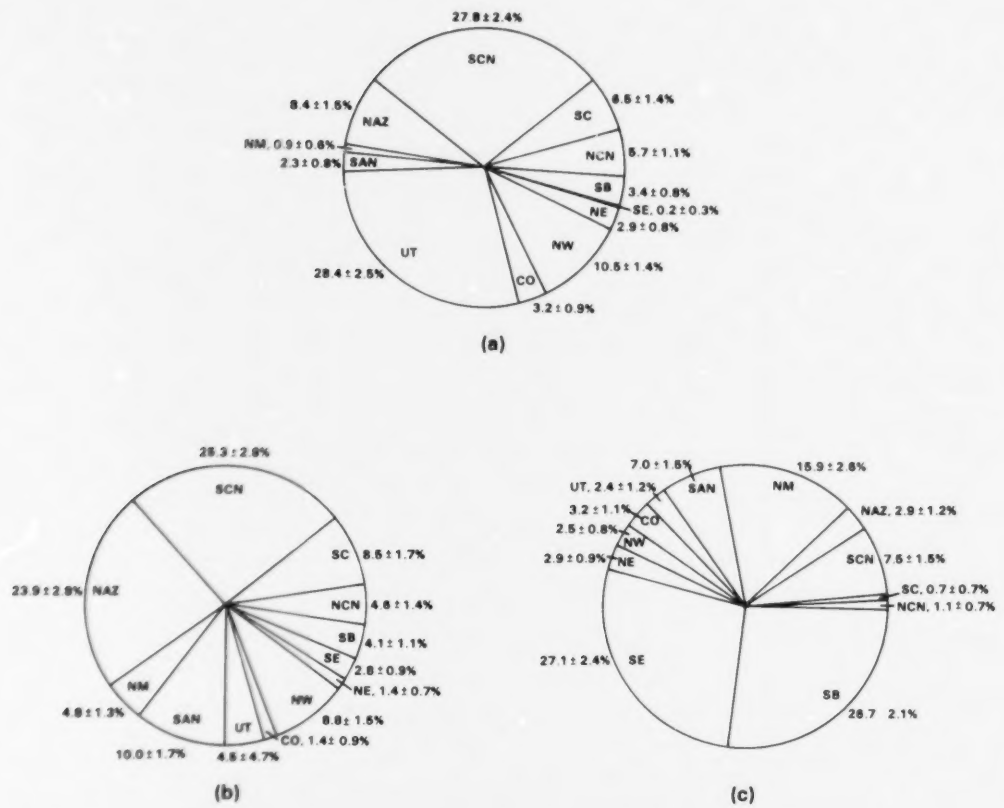

Fig. 6(a–c). Two-year mean transport extinction budgets for 'North', 'Center' and 'South' groups, respectively. Mean plus or minus standard error contributions in percentages.

contribution from the window containing the trajectory end point provides a substantial fraction of the group mean extinction coefficients. Perhaps the local impacts on extinction are reflected to some degree in these end-point windows. For both the 'North' and 'Center' the SCN and SC contributions amount to about one-third of the total which is about 4 times their contribution to the 'South'. The contributions of SAN are similar for the 'Center' and 'South' groups and about 3–4 times larger than for the 'North'. The contribution of SE and SB windows, not surprisingly, increases from being nearly inconsequential in the 'North', through small in the 'Center' to dominant in the 'South'.

The extinction-contribution pie diagrams look similar to pie diagrams of the mean residence time for each window (not shown). This is due to the relatively narrow distribution in the set of regression coefficients (C_{ij}) compared to the distribution in the set of mean residence times. Thus although there are differences in the extinction per unit residence time (Figs 5a–c), it is the 2-year average residence time distribution (shown in Table 5) which is most influential in determining the overall extinction contribution distribution (Figs 6a–c).

The regression technique provides a means to assess the predictive capability of the models presented above. The standard errors of estimate (standard deviation of ε) for the 'North', 'Center' and 'South' groups are 0.0106 km^{-1}, 0.0136 km^{-1} and 0.0142 km^{-1}, respectively. These values are unacceptably high for prediction purposes. Thus knowledge of the trajectory of an air parcel cannot be used alone to estimate daily visibility levels. In spite of this, the models have provided useful information concerning the long-term average influence of upwind areas (windows) on visibility. The impacts of other factors, along with measurement error and errors caused by misdetermined trajectories, are responsible for the large standard errors of estimate. The C_{ij} terms also incorporate some of the non-transport factors, to the extent to which their influence is associated with transport. For example, if high relative humidity and precipitation are associated with certain windows more than others, then the visibility effects of these factors are incorporated into the regression coefficients.

Though the model results presented in this work provide no means to assess the relative influence of non-transport factors, the models do suggest methods for investigating these factors. Meteorological and

pollutant source factors for days where the model performed well can be compared with those for days when it either greatly over- or under-predicted the measured visibility. Parameters of importance, identified in this way, can be incorporated into the model development and evaluation process. Another aspect of the present model which can be evaluated and optimized is the number, size, shape and location of the windows used. It is expected that using these approaches will result in a lowered standard error of estimate, more precisely defined regression coefficients and a greater understanding of regional visibility degradation.

SUMMARY AND CONCLUSIONS

1. Principal component analysis applied to visibility data from 13 locations in the desert southwest indicates for each season there are three to four regions, within which visibility is similarly varying.

2. In each season, a 'North', 'Center' and 'South' region of similarly varying visibility can be identified. They are in eastern Utah, northern and eastern Arizona and New Mexico, respectively. The size, shape and location of these varies somewhat from one season to the next and hence they are referred to as the 'North', 'Center' and 'South' groups (each group contains four seasonal regions).

3. Of the three groups, long-term mean visibility is greatest for the 'North' and lowest for the 'South'. The 'Center' and 'South' groups have a distinctive and large annual visibility cycle with best visibility in the winter and poorest in the summer. Short-term (one to several days) visibility variations are often greater than mean seasonal changes for each group.

4. Methods were developed to summarize and exploit two years of back trajectory data in order to investigate the relationship between visibility and transport for the three groups. These methods were based upon the premise that the influence of an area on the air quality of an air parcel moving over it is related to the length of time the air spent over the area.

5. The fraction of back-trajectory time from the west is 85, 75 and 65% for the 'North', 'Center' and 'South' groups, respectively. This decreasing trend through the groups is primarily caused by less time spent in the southwest quadrant with corresponding greater time spent in the east (primarily the southeast).

6. A method to estimate the long-term average transport contribution to extinction from arbitrarily defined upwind areas was developed based upon statistical relationships between group visibility and the time trajectories spent in the upwind areas (residence time). The analysis indicated many of the areas to have statistically similar extinction per residence time. The extinction contributions summarized below are thus similar to the fractional residence time for each area.

7. Mean transport extinction budgets for the three groups indicate one-third contribution to 'North' and 'Center' groups extinction coefficient from Southern California (SCN and SC), which is about 4 times its contribution to extinction for the 'South'.

8. Contributions from the southeast (SE) and south of the US/Mexican border (SB) contribute about 54, 7 and 3% of the 'South', Center' and 'North' groups extinction coefficients, respectively.

9. The region of Southern Arizona and New Mexico which contains the copper smelting industry contributes nearly 10, 7 and 2% of the extinction for the 'Center', 'South' and 'North' groups, respectively.

10. Judging by the extinction associated with the area containing the trajectory end points for three groups, the contribution from local sources is substantial (28% for UT-'North', 24% for NAZ-'Center' and 16% for NM-'South').

REFERENCES

Allard D., Tombach I., Mayrshon H. and Mathai C. V. (1982) Aerosol measurements: western regional air quality studies. Paper No. 82-39.2 presented at the 75th Annual Air Pollution Control Association Meeting, New Orleans, Louisiana.

Ashbaugh L. L. (1983) A statistical trajectory technique for determining air pollution source regions. *J. Air Pollut. Control Ass.* **33,** 1096.

Ashbaugh L. L., Myrup L. O. and Flocchini R. G. (1984) Principal component analysis of sulfur concentrations in the western United States. *Atmospheric Environment* **18,** 783–792.

Bevington P. R. (1969) *Data Reduction and Error Analysis for the Physical Sciences.* McGraw-Hill, New York.

Blumenthal D. L., Richards L. W., Macias E. S., Bergstrom R. W., Wilson W. E. and Bhardwaja P. S. (1981) Effects of a coal fired power plant and other sources on southwestern visibility (interim summary of EPA's project VISTTA). *Atmospheric Environment* **15,** 1955–1970.

Dixon W. J. and Brown M. B. (eds.) (1977) *BMDP-77 Biomedical Computer Programs P Series.* University of California Press, Berkeley, California.

Galvin P. J., Sampson P. J., Coffey P. E. and Romano D. (1978) Transport of sulfates to New York State. *Envir. Sci. Technol.* **12,** 580.

Hall F. P., Jr., Duchon C. E., Lee L. G. and Hagan R. R. (1973) Long-range transport of air pollution: a case study, August 1970. *Mon. Weath. Rev.* **101,** 404.

Hansen D. A. and Watson J. G. (1983) Draft program plan for the Subregional Cooperative Electric Utility, National Park Service, and Environmental Protection Agency Study (SCENES). ERT document No. P-A765-600-E.

Heffter J. L. (1980) Air resources laboratories atmospheric transport and dispersion model (ARL-ATAD). NOAA, Tech. Memo ERL ARL-81. Air Resources Laboratories, Silver Spring, Massachusetts.

Heffter, J. L., and Ferber, G. J. (1977). Development and verification of the ARL regional–continental transport and dispersion model. In *Proceedings of the Joint Conference on Application of Air Pollution Meteorology,* American Meteorological Society, Boston, Massachusetts.

Hoffer T. E., Miller D. F. and Farber R. J. (1981) A case study of visibility as related to regional transport. *Atmospheric Environment* **15,** 1935–1942.

Horel J. D. (1981) A rotated principal component analysis of the interannual variability of the northern hemisphere

500 mb height field. *Mon. Weath. Rev.* **109,** 2080.
Kidson J. W. (1975) Eigenvector analysis of monthly mean surface data. *Mon. Weath. Rev.* **109,** 177.
Kutzback J. E. (1970) Large-scale features of monthly mean northern hemisphere anomaly maps of sea level pressure. *Mon. Weath. Rev.* **98,** 708.
Malm W. C. Walther E. G., O'Dell K. and Kleine M. (1981) Visibility in the southwestern United States from summer 1978 to spring 1979. *Atmospheric Environment* **15,** 2031–2042.
Miller J. M. (1981a) A 5-year climatology of 5-day back trajectories from Barrow, Alaska. *Atmospheric Environment* **15,** 1401–1407.
Miller J. M. (1981b) A 5-year climatology of back trajectories from the Mauna Loa Observatory, Hawaii. *Atmospheric Environment* **15,** 1553–1559.
Miller J. M., Galloway J. N. and Likens G. E. (1978) Origin of air masses producing acid precipitation at Ithaca, New York, a preliminary report. *Geophys. Res. Lett.* **5,** 757.
Pitchford A., Pitchford M., Malm W., Flocchini R. and Cahill T. (1981) Regional analysis of factors affecting visual air quality. *Atmospheric Environment* **15,** 2043–2054.
Raynor G. S. and Hayes J. V. (1982) Effects of varying air trajectories on special and temporal precipitation chemistry patterns. *Water Air Soil Pollut.* **18,** 173.
Raynor G. S., Hayes J. V. and Lewis D. M. (1983) Testing of the Air Resources Laboratories trajectory model on cases of pollen wet deposition after long-distance transport from known source regions. *Atmospheric Environment* **17,** 213–220.
Sampson P. J. (1981) Trajectory analysis of summertime sulfate concentrations in the northeastern United States. *J. appl. Met.* **19,** 1382.
U.S. EPA (1983) Western regional visibility monitoring: teleradiometer and camera network, TS-AMD-8035b. Environmental Monitroing Systems Laboratory, Las Vegas, Nevada.
Walsh J. E. and Mostek A. (1980) A quantitative analysis of meteorological anomaly patterns over the United States 1900–1977. *Mon. Weath. Rev.* **108,** 615.
Wolff G. T., Lioy P. J., Wight G. D., Meyers R. E. and Cederwall R. T. (1977) An investigation of long-range transport of ozone across the mid-western and eastern United States. *Atmospheric Environment* **11,** 797–802.

NOTICE

This document has been reviewed in accordance with U.S. Environmental Protection Agency policy and approved for publication. Mention of trade names or commercial products does not constitute endorsement or recommendation for use.

This article documents research that was conducted under the auspices of the U.S. Environmental Protection Agency (USEPA). As an arm of the government, the USEPA has a paid up, non-exclusive, irrevocable, worldwide license to reproduce, prepare derivative works, and distribute to the public all of the material contained herein, and to grant others acting on its behalf the right to do so. The USEPA grants to the National Technical Information Service, Department of Commerce, the right to act as its agent in the distribution of this material.